JME

*J*ournal of *M*ining & *E*nvironment,
Vol.8, No.1, 2017, 111-130.
*DOI: 10.22044/jme.2016.573*

# Evaluation of structural analysis of tunnel segmental lining using beam-spring method and force-method (Case study: Chamshir water conveyance tunnel)

M. Nikkhah[1*], S.S. Mousavi[1], Sh. Zare[1] and O. Khademhosseini[2]

*1. School of Mining, Petroleum & Geophysics Engineering, Shahrood University of Technology, Shahrood, Iran*
*2. School of Civil Engineering, Shahrood University of Technology, Shahrood, Iran*

Received 20 November 2015; received in revised form 21 January 2016; accepted 25 January 2016
**Corresponding author: m.nikkhah@shahroodut.ac.ir (M. Nikkhah).*

## Abstract
The joints between segmental rings can withstand a certain amount of bending moment as well as axial and shear forces. Generally, in the structural analysis of tunnel segmental lining, the joints can be modeled as elastic hinges or rotational springs, and their rigidity should be demonstrated in terms of the rigidity of the joints or their rotational stiffness. Therefore, the bending moment acting on the tunnel lining is reduced. Hence, the tunnel designers are free to choose a lining with a lower cost. In this research work, especially considering the joints, the structural analysis of the segmental lining with variation in the flexural stiffness of the joints ( $\lambda$ ), soil resistance coefficient ( $K_S$ ), number of segmental lining joints, and joint arrangement of segmental lining were carried out by the Force-Method equations. The imposed bending moment and axial forces were computed based on the Beam-Spring method, which is widely used to analyze the internal forces of segmental lining, and compared them with the results of the Force-Method equations. Then the effects of joint arrangement patterns and joint rotational spring stiffness on the results of the Beam-Spring analysis were evaluated. Finally, the optimum characteristics of the reinforced concrete segmental lining design were evaluated using the interaction diagram of bending moments and axial forces. The results obtained showed that the presented pattern for the segmental lining at the Chamshir tunnel was imposed against the external pressures on the segmental lining with an acceptable safety factor.

**Keywords:** *Tunnel, Design of Segmental Lining, Structural Analysis, Beam-Spring Method, Chamshir Tunnel.*

## 1. Introduction
With the development of shield-driven machines and the advancement of construction technology, the diameters of these tunnels may run the gamut from about 5 m to more than 12 m. The compatibility of shield-driven tunnels has been improved by various intricate and difficult geological conditions. In most shield-driven tunnels, the connected jointed segmental precast concrete linings are commonly used by the steel bolts instead of the steel or cast iron segments. Although the lining of a shield-driven tunnel is not a continuous ring structure due to the existence of joints, the effect of joints on the internal forces and displacements should be considered in the lining design. Generally, the influence of joints on the bending moment and axial forces is one of the main elements in the segmental lining design of shield-driven tunnels. It happens due to the difference between the joint and segment rigidity in the continuous form structure. Recent research works have indicated that the segment joint has a maximum deflection compared to the main body. Thus the designers have assumed the hinges of segments as a critical part of segment in the design. The cover of tunnels usually has been considered by a

dimensionless parameter called the flexural stiffness coefficient, which was presented and completed by Peck and Einstein in 1972 and 1979. The flextural stiffness coefficient indicates the relationship between the host rock and the structural features of the support system. Flextural stiffness plays an important role in the stability of tunnel lining. In fact, the internal bending moment would be decreased by increasing the flextural stiffness. This coefficient is defined by the following equation [1, 2]:

$$F = \frac{\frac{E_S}{(1+\upsilon_S)}}{\frac{6EI}{(1-\upsilon^2)}} \quad (1)$$

where $E_S$, $\upsilon_S$, $E$, $I$, and $\upsilon$ are the Young's modulus of rock mass, Poisson's ratio of rock, Young's modulus of lining, moment inertia of lining, and Poisson's ratio of lining, respectively.

In 1975, Wood proposed that the effective moment inertia of the segmental lining should be revised according to the following equation [3]:

$$I = \left(\left[\frac{4}{N'}\right]^2 \times I_O\right) + I_j \quad (2)$$

where $I_O$ and $I_j$ represent the moment inertia of lining without joints (continuous lining) and moment inertia of lining in joint position, respectively.

Wood has also found that the presence of joints does not affect the rigidity of lining for four or fewer lining segments. The earth pressure acting around a tunnel has been assumed to be an elliptical shape in this model. To obtain the elliptical shape of the initial loading, we need a sufficient overburden thickness [3]. Therefore, Wood's model is more applicable to deep tunnels since the assumption may not be valid for shallow tunnels. In 1996, Bickel et al. have proposed a 2D model to simulate the segment joints using lower stiffness parameters [4]. This model assumes that the stiffness (effective modulus of the elasticity) of a segmental ring is half of a monolithic ring by the inertia moment of the practical coffered precast segments ranging from 60-80% of those solid sections with the same thickness. In the wake of the reduced stiffness, this model is more flexible than the continuous lining, and is expected to yield less values for the bending moment and hoop forces. Furthermore, Koyama and Nishimura (1998) have developed a model similar to the former model by Bickel et al. [5].

According to this model, the tunnel lining is assumed to be a continuous ring with a discounted rigidity by applying a reduction factor η value to the bending rigidity ($EI$) of lining. Koyama and Nishimura (1998) found η after a full-ring structural testing. In the absence of the experimental data, the value for $\eta$ could be assumed to be in the range of 0.6-1.0 for the preliminary design analysis [5]. For instance, in 1992, Uchida presented a continuous monolithic ring beam with a constant effective rigidity ratio of $\eta = 0.8$, which was used in the design of the Trans-Tokyo Bay Highway tunnel lining [6].

The η value adopted in the tunnel project was later verified by tests on a full-scale prototype segmental lining. Lee and Ge (2001) have presented an analytical correlation between the effective moment inertia and the maximum horizontal displacement of a continuous lining structure, as follows [7]:

$$\eta = \frac{1}{1+\Delta_h} \quad \Delta_h = \frac{3EI}{R \times K_\theta} \times \sum_{i=0}^{N'} \cos\varphi_i \times \cos 2\varphi_i \quad (3)$$

where $N'$, $K_\theta$, $R$, $\varphi_i$, $\eta$, and $\Delta_h$ are the numbers of segment pieces, flextural stiffness of lining joints, external radius of tunnel lining, angle of the $ith$ joint relative to the tunnel crown, reduction factor of the bending moment, and horizontal displacement of lining, respectively.

An analytical solution has been presented by Lee et al. (2001) based on the Force-Method and energy equation for simulating segmental lining in terms of lining joints. In their research work, the rigidity of joints was simulated as an elastic hinge with constant rigidity [8]. Koyama (2003), by drawing on the design experience of Japanese civil engineers, has demonstrated that the superlative bending moment imposed on the lining was 60-80% of the superlative bending moment imposed on the continuous lining structure in designing a segmental lining relative to the joints [9]. Lu et al. (2006) have examined the act of a segmental lining by excluding the effect of joints. They have evaluated the effects of imposed loading (bending moment, axial forces, and shear forces) on the joint of a segmental cover using the PLAXIS software based on the finite element method [10]. Teachavorasinkun and Chub (2010) have performed an experimental research work to find 4 segmental models consisting of two segments with joints and two continuous segments

with different thicknesses. They concluded that the coefficient of bending moment depended heavily on the strength of segmental lining joints [11]. On the other hand, they found that there was a direct correlation between the bending moment coefficient and the joint strength.

Arnau and Molins (2012) have analyzed the influence of the interaction between adjacent rings in the structural response of segmental tunnel linings when they were subjected to typical design loads (longitudinally uniform) [12]. In this research work, they performed a real scale test on an experimental tunnel section of the new Line 9 of the Barcelona underground metro system. The section composed of 15 rings built using only steel fibers as the reinforcement. The contact between the longitudinal joints was modelled using unilateral interface elements located on one side of the plastic packer elements. The measurements and results of the numerical simulation were similar in terms of displacements, joint closures, and crack patterns.

They have also presented a theoretical analysis of the structural resistant mechanisms to establish the main parameters involving the 3D responses of the tunnel linings. Thus they accomplished a 3D finite element model of a real tunnel section by applying the modeling techniques that allowed the simulation of both the joint responses and the material behavior. They concluded that increasing the internal forces generated by coupling effects could produce the segment cracking, reducing the lining stiffness, and behaving between a rigid pipe and an isolated ring [13, 14].

Do et al. (2013) have presented a 2D numerical analysis of the segmental tunnel lining behavior, in which the effects of the joint stiffness, Young's modulus of the ground, and lateral earth pressure factor were considered by a finite difference element program [15]. They examined the influence of certain characteristics including the rotational stiffness, axial stiffness, and radial stiffness of longitudinal joints on the tunnel behavior regarding the effect of packing material to simulate the interaction between the tunnel lining and the surrounding medium in a more realistic way [15].

Li et al. (2015) has investigated the development of longitudinal joint opening with both sagging moment (i.e. positive bending moments) and hogging moment (i.e. negative bending moment) under different axial stress levels. In this research work, the authors first conducted full-scale tests on the longitudinal joint adopted by the Shanghai Metro Line No. 13. Then a progressive model was presented to simulate the joint opening behavior based on the test observations for verification of the test results [16]. In this research work, we examined the longitudinal joint opening in the Ultimate Limit State (ULS), which had not been obtained by the previous tests [17-19].

In the current study, first the internal forces were calculated in terms of joints of lining. Then an analytical solution was carried out for the structural analysis of the segmental joints and its displacement using the Force-Method equations with changes in the flexural stiffness of the joints (λ), rock resistance coefficient (Ks), number of segmental lining joints, and joint arrangement that uses elastic hinges for simulating the joints behavior. Consequently, the imposed bending moment and axial forces were computed based on the Beam-Spring method by means of the rotational and radial stiffness as well as the ground-structure interaction to define the boundary condition of the structure. Then together with comparing the results obtained for the two approaches, the effects of joint arrangement pattern and joint rotational spring stiffness were evaluated on the result of the Beam-Spring analysis. Finally, the optimum segmental lining design was assessed by means of the axial forces *vs.* bending moment interaction curve.

## 2. Evaluation of internal forces

### 2.1. Force-Method

A jointed shield-driven tunnel lining embedded in soil and rock is a redundant structure. Since most segmental concrete lining systems are waterproofed by gaskets at the joints, the lining structures are usually subjected to both the earth and water pressures. Therefore, the earth pressure distribution and the structural responses of the segmental lining structure are subjected to overall stresses. According to the field observation of the earth pressure distributions acting around the segmental lining, the earth pressure can be expressed as shown in Figure 1, where:

$P_1$: Vertical overburden earth pressure;

$P_2$: Reaction pressure at the bottom of lining;

$P_3$: Total lateral earth pressure developed at the crown level of tunnel lining;

$P_4$: Lateral earth pressure developed at the tunnel invert level;

$P_5$: Self-weight of tunnel lining;

$P_6$: Rock/soil resistance pressure.

Here, $P_6$ was assumed to be distributed over a range of 45-135 degrees with respect to the vertical direction around the tunnel acting perpendicular to the tunnel with a parabolic pattern, as defined by the following equation [8]:

$$P_6 = P_h \times \left(1-(2cos^2\varphi)\right) \quad (3)$$

Here, $P_h$ is the rock/soil resistance developed at the spring line of the tunnel, and $\varphi$ is the angle measured using the vertical direction around the tunnel. By adopting Winkler's type of soil/rock reaction, $P_h$ can be calculated as follows [8]:

$$P_h = K_s \times \Delta_h \quad (4)$$

where $K_S$ is the soil/rock resistance coefficient, and $\Delta_h$ is the horizontal displacement at the spring line of the tunnel.

In this research work, a computer program was designed by the MATLAB software to solve the proposed analytical equations. Since the horizontal displacement at the spring line is unknown at the outset, the soil/rock reaction had to be determined by iterations. The flowchart of the iteration process is shown in Figure 2.

The aim of this part of the work was to evaluate the internal forces of the Chamshir water conveyance tunnel by changing the flexural stiffness for the joints ($\lambda$),soil resistance coefficient ($K_S$),number of segmental joints, and joint arrangement of segmental lining.

The Chamshir dam is located in the SW of Iran, and is mainly used for the purpose of water supply and irrigation (see Figure 3). In this project, a 7.1-Km tunnel was excavated by a tunnel boring machine (TBM). The geo-mechanical properties of rock mass and the mechanical and geometrical properties of segmental lining are depicted in Tables 1 and 2, respectively.

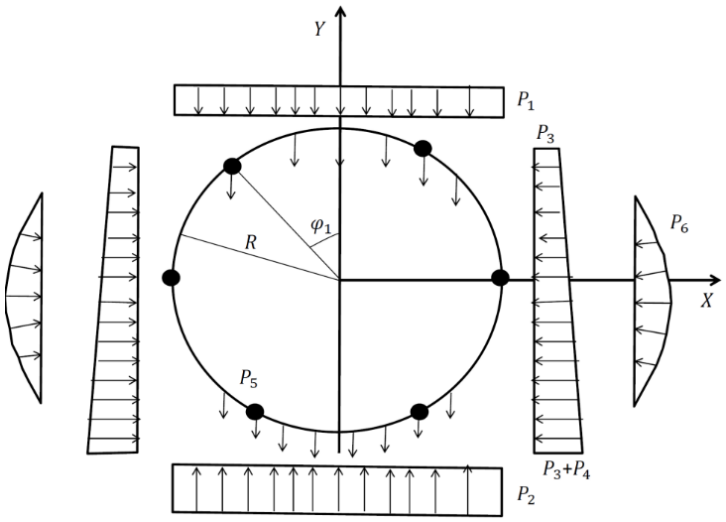


**Figure 1. Model diagram of a jointed tunnel lining [7, 8].**

**Table 1. Geo-mechanical properties of rock mass.**

| Density (kg/m$^3$) | Elastic modulus (GPa) | Friction Angle (degree) | Cohesion (MPa) |
|---|---|---|---|
| 2.7 | 1.323 | 28.5 | 0.3 |

**Table 2. Properties of segmental lining.**

| Parameter | Value | Parameter | Value |
|---|---|---|---|
| Density ($kg/m^3$) | 2400 | Elastic modulus of concrete (MPa) | 35 |
| Internal radius (m) | 2.5 | Design compressive strength of concrete (MPa) | 33 |
| Thickness (m) | 0.25 | Elastic modulus of reinforcements (MPa) | 200 |
| Width of segment (m) | 1.2 | Design strength of reinforcement (MPa) | 350 |

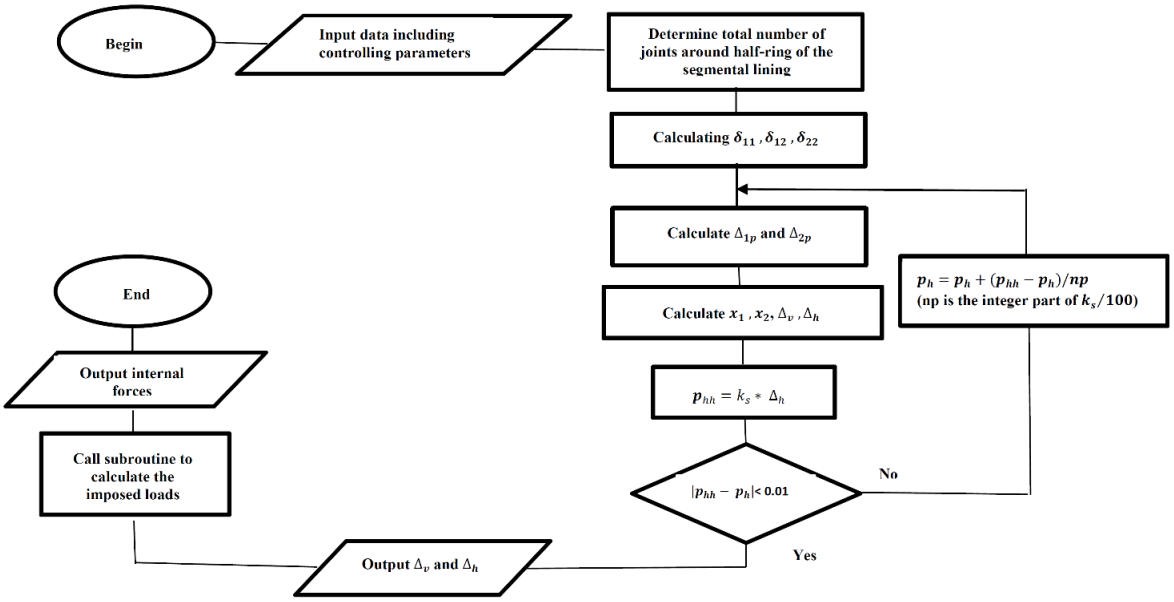


**Figure 2. Flowchart of computer program [8].**

### 2.1.1. Effect of flexural stiffness of joints

A reduction in the amount of joint flexural stiffness can reduce the bending moment. Also with a decline in the flexural stiffness, the deformation of segments and the imposed soil/rock resistance pressure would be increased as well. As a result, the imposed axial forces will be increased.

In this work, for a better understanding of the joint effect on the internal forces, the bending moment and axial forces of the Chamshir segmental tunnel lining with 6 lining joints were analyzed based on the Force-Method equations for the three cases $\lambda = 1$, $\lambda = 0.1$, and $\lambda = 0.01$, as depicted in Figures 4 and 5, respectively. The joint stiffness coefficient is defined as the ratio of flexural stiffness of the joints to the flexural rigidity of lining ( $\lambda = K / EI$ ). As shown in Figure 4, the bending moment dropped when the joint stiffness coefficient was less than 1. On the other hand, when the rigidity of joints increased, the lining behavior remained closed to continuous form thereby increasing the bending moment.

Also, as illustrated in Figure 5, the axial forces of lining increased for the joint stiffness coefficients lower than 1. Figure 6 shows the variations in the vertical and horizontal displacements of the tunnel with different values of joint stiffness. As it can be seen, with decrease in the joint stiffness coefficient, the vertical and horizontal displacements of segmental lining increased. More horizontal and vertical displacements were observed for the joint stiffness coefficients less than 0.1.

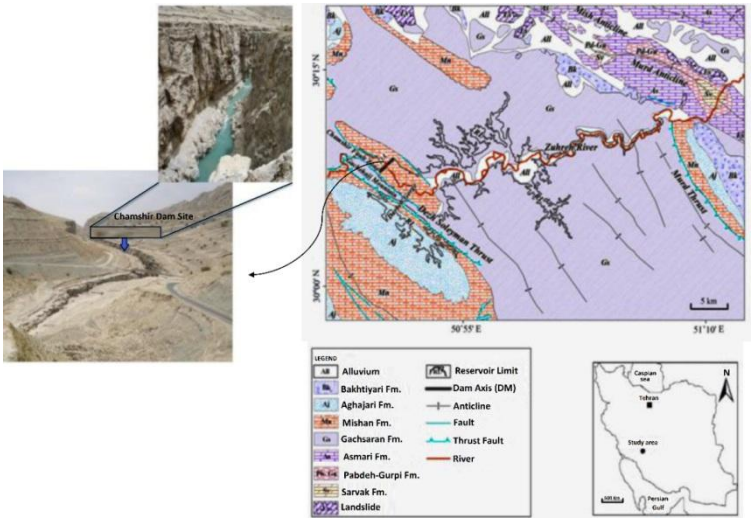


**Figure 3. Geological map of studied area [20].**

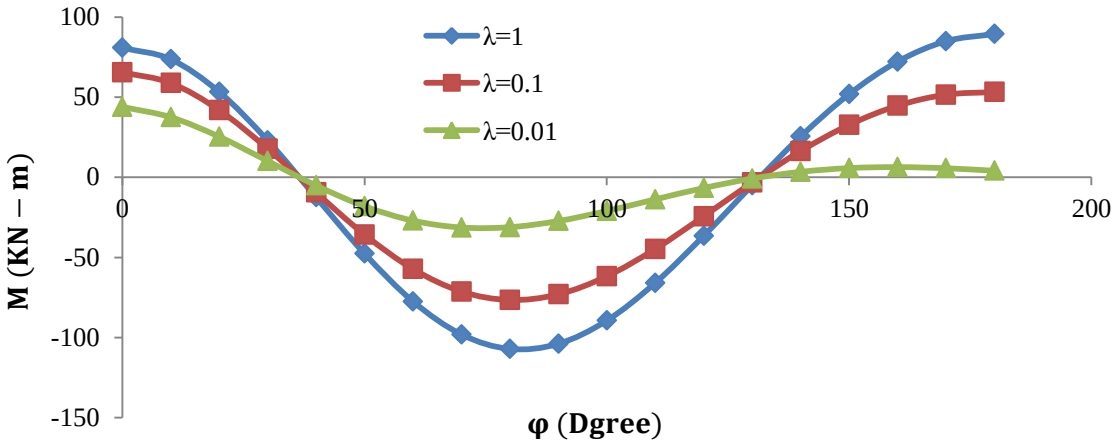


**Figure 4. Variation in bending moment versus angle based on measurement of vertical pressure around tunnel for different joint stiffness values.**

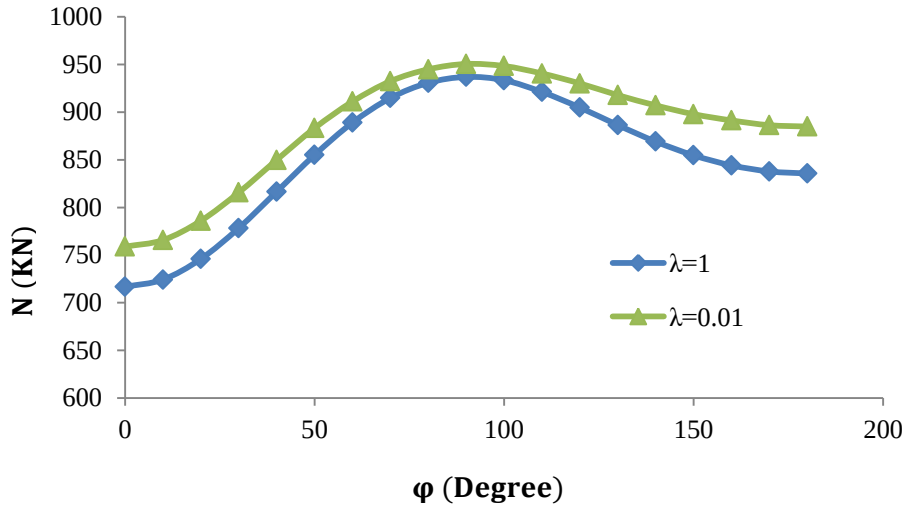


**Figure 5. Variation in axial force versus angle based on measurement of vertical around tunnel for different joint stiffness values.**

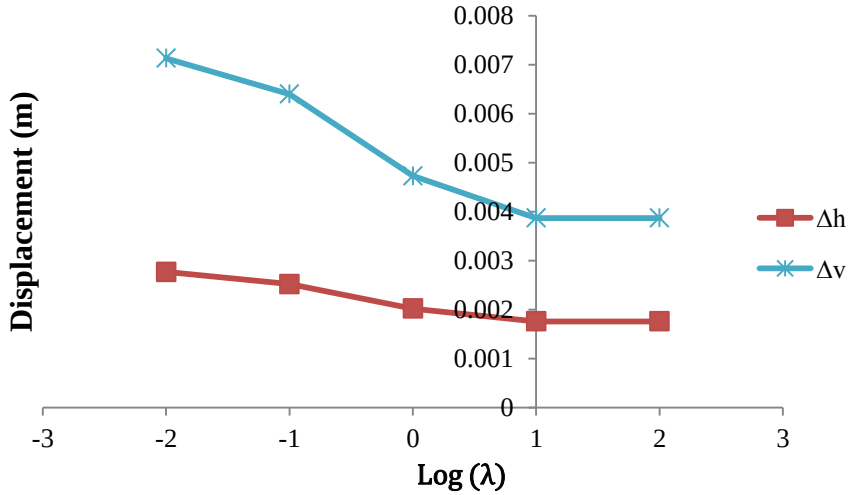


**Figure 6. Variation in vertical and horizontal displacements with different joint stiffness values.**

### 2.1.2. Effect of rock resistance coefficient ($K_s$)

In fact, by increasing the soil/rock resistance coefficient, the rock strength specification is improved. Hence, with an increase in the $K_S$ value, the deformation of segmental lining is decreased. Also by increasing the soil resistance coefficient, the bending moments are reduced, while the imposed rock resistance pressure rises. As a result, the imposing axial forces on the segmental lining increase as well. This is depicted in Figures 7 and 8 for the Chamshir tunnel segmental lining containing 6 joints.

As shown in Figures 7 and 8, an increase in the soil/rock resistance coefficient rises the imposed bending moments and reduces the imposed axial forces. In this analysis, the joint stiffness was considered equal to the segmental lining rigidity ($\lambda = 1$).

The correlation between the tunnel displacements against the joint stiffness and rock stiffness coefficient are shown in Figure 9. As it can be seen, the vertical and horizontal displacements against the joint stiffness in zero rock resistance coefficients are more sensitive than the other coefficients. Hence, it indicated more displacements in this value.

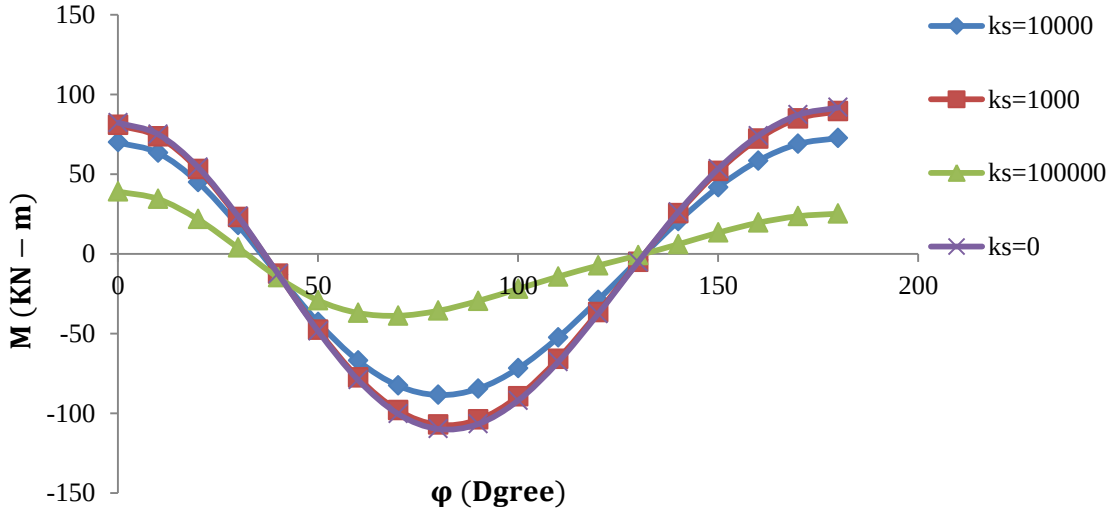


**Figure 7. Variation in bending moment by different soil/rock resistance coefficient values.**

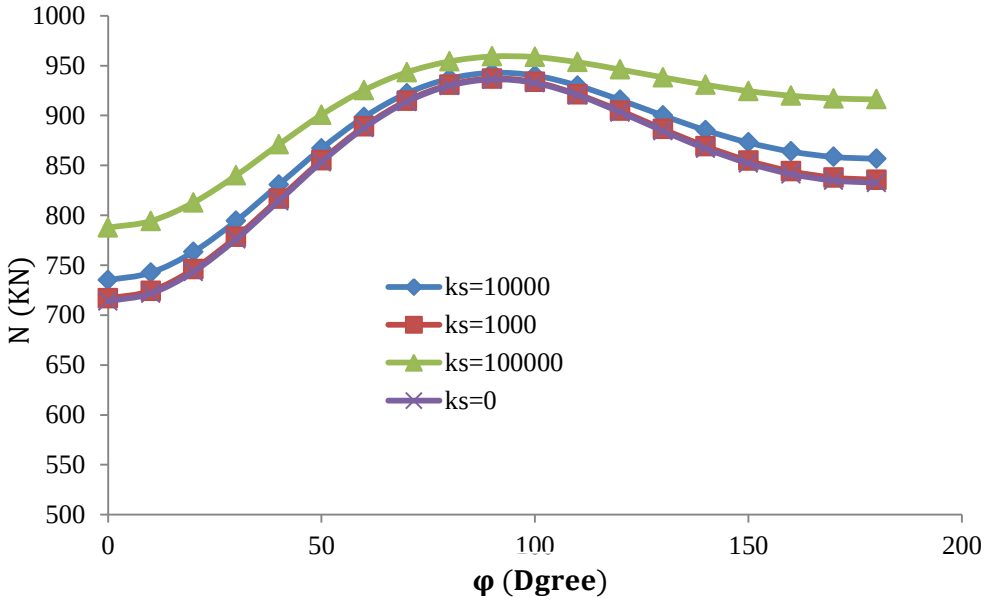


**Figure 8. Variation in axial forces by different soil/rock resistance coefficient values.**

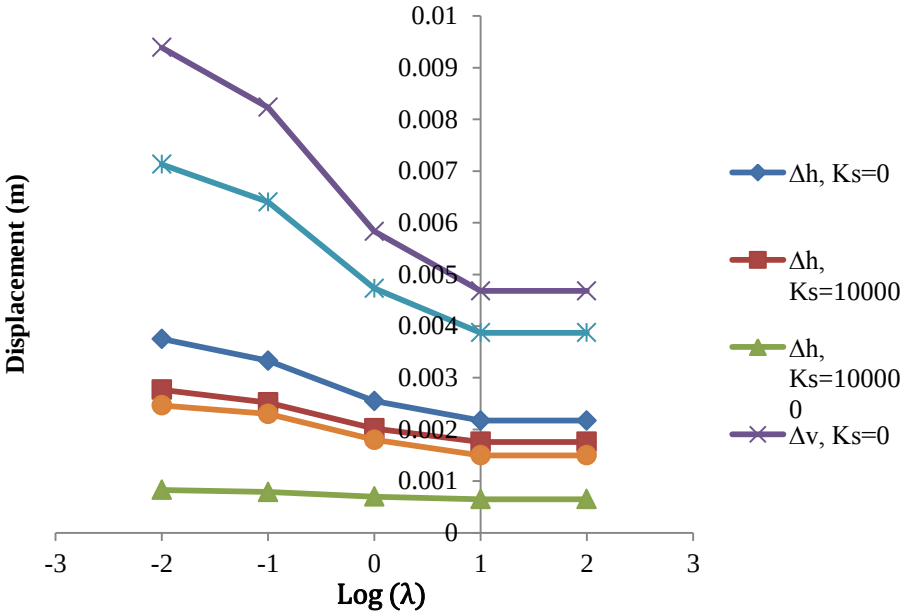


**Figure 9. Segmental lining displacement by different rock resistance coefficient values.**

### 2.1.3. Effect of joint number

As the joint number rises, the flexibility of segmental lining is increased, leading to a decline in the bending moments. However, an increase in the number of joints augments the lining deformation and the rock reaction pressure. On the other hand, the imposed axial forces, which are extremely affected by pressure, are increased as well. Figures 10 and 11 show variations in the bending moments and axial forces.

In these figures, the internal forces of two types of segments with 6 and 8 lining joints have been compared for three types of flexural stiffness ($\lambda = 0.1$, $\lambda = 0.01$, and $\lambda = 1$).

As shown in Figure 12, it seems that an increase in the number of lining joints raises the displacement of the segmental lining. In addition, the vertical displacement growth of the segmental lining is more significant when the ratio of lining joint rigidity versus segmental lining rigidity is less than 0.1.

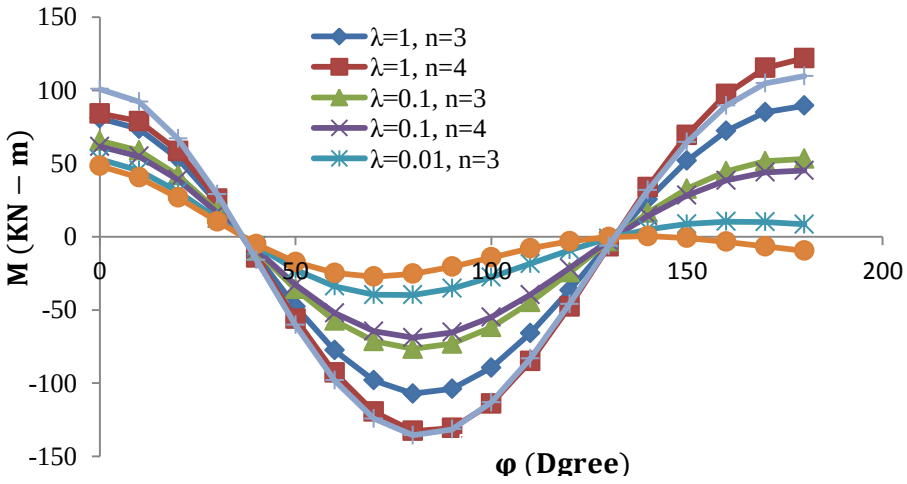


**Figure 10. Variation in bending moment by number of lining joints.**

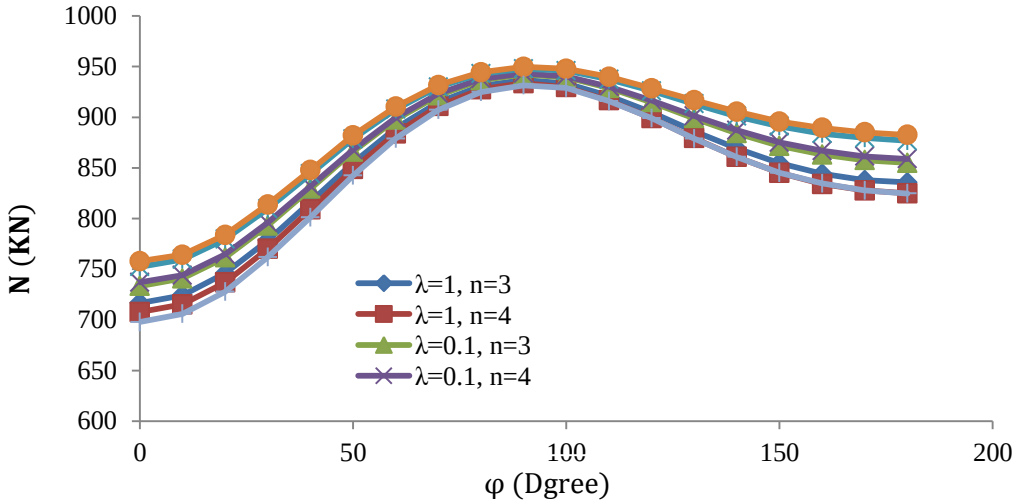


**Figure 11. Variation in axial forces by number of lining joints.**

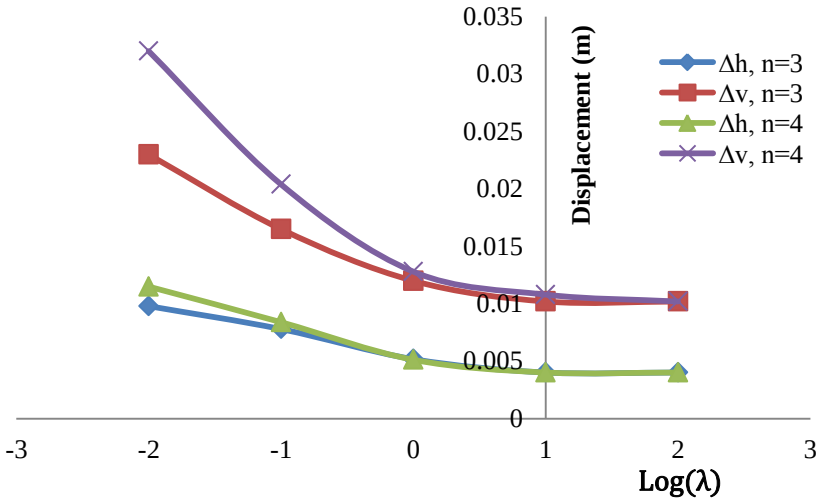


**Figure 12. Variation in segmental lining displacement by number of lining joints.**

### 2.1.4. Effect of segmental lining joint arrangement

To assess the effect of joint arrangement on the bending moment and axial forces of the Chamshir water conveyance tunnel, two types of arrangements (chosen from other projects) with different joint angle measurements were studied for a lining of 8 segmental pieces as follows:

Case 1: 38, 83, 128, 173, 218, 263, 308, 353 degrees.

Case 2: 5, 50, 95, 140, 185, 230, 275, 320 degrees.

For each type of joint arrangement, the imposed bending moment and axial forces were calculated, as illustrated in Figures13 and 14.

As shown in these figures, with an increase in the lining joint angle (with regard to the tunnel crown), the bending moment and axial forces rise and fall, respectively. Hence, when the joint is located near the tunnel crown, the lining joint arrangements will have an optimal arrangement from a structural viewpoint. The displacement of these two joint arrangement patterns is shown in Figure 15. As it can be seen, the horizontal displacements derived from the analysis of lining joint arrangements do not change significantly. In the case of the second lining joint arrangement, however, the vertical displacement changes are remarkable, particularly when the joint stiffness of segmental lining is less than 0.1 of the segmental lining rigidity.

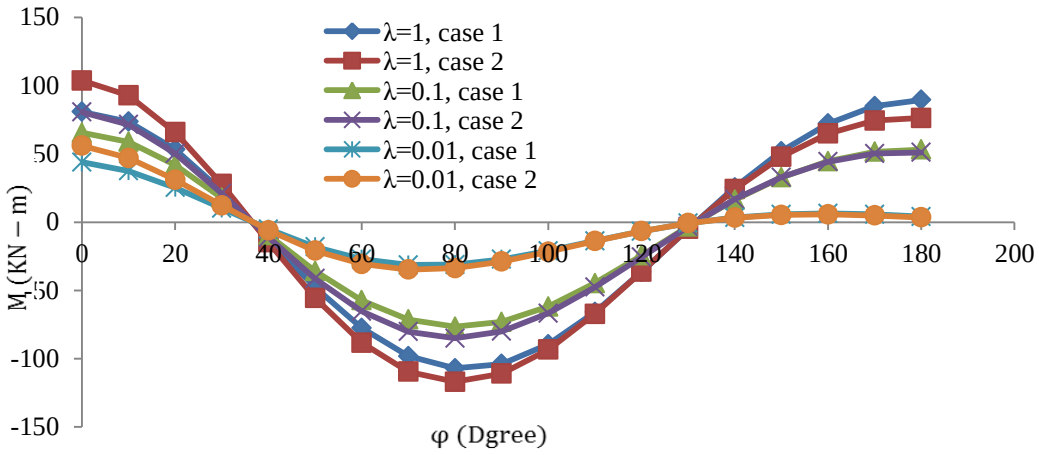


**Figure 13. Variation in bending moment by different joint arrangements.**

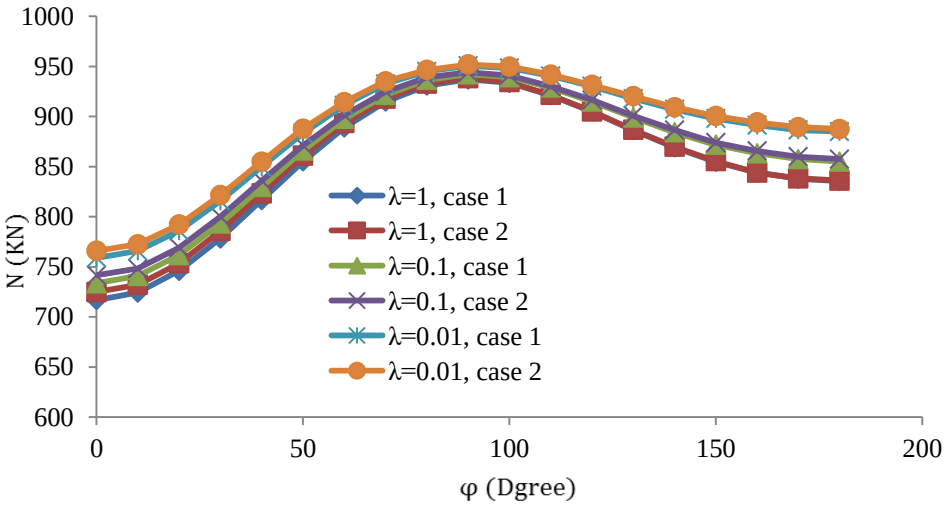


**Figure 14. Variation in axial forces by different joint arrangements.**

## 3. Beam-Spring method

The Beam-Spring method, known as "the coefficient of subgrade reaction method", is illustrated in Figure 16. In this method, the lining is generally represented by an arc, which is reduced to a polygon with fixed angles. Each piece of lining is supported by springs, whose elasticity represents the ground reaction. In other words, the lining and ground are represented by a series of beams and springs, respectively. It is assumed that the ground reaction is generated by the displacement of the lining proportional to the ground deformation [21]. This assumption accounts for the interaction between the segments and the surrounding ground.

In the application of this method, the ground springs are commonly assumed to affect the radial direction but there are cases in which they have been reported to affect the tangential direction [22]. To achieve more conservative (safe) results, only the rock springs acting on the radial direction are used to represent the surrounding ground. This assumption indicates the frictionless sliding of the lining against the ground.

The structural analysis by the Beam-Spring method is also based upon the assumption that the rock reaction forces are activated when the tunnel expands outward but they are not activated when the tunnel contracts inward. For this reason, the non-tension ground springs are used to represent the interaction between the lining and the surrounding ground. Segmental rings are generated by assembling several segments with bolts or dowels. The rigidity of connection joints between the segments is lower than that for the main section of the segment. Therefore, the deformation of a segmental ring tends to be larger than that for a ring with a uniform bending rigidity. At this point, the evaluation of the

reduced rigidity at joints is of importance in calculating the member forces. For this purpose, various 2D approaches have been developed to evaluate the segmental joints. In this sense, there are several design models that assume the segmental ring as a solid ring with fully bending rigidity, a solid ring with reduced bending rigidity, a ring with multiple hinged joints, a ring with rotational springs, etc. [22, 23].

Since the Beam-Spring method is the most effective and practical tool to calculate the member forces of the TBM segmental linings, several theoretical approaches have been proposed in this field. The main determinants in Beam-Spring are the ground lining interaction and connection joints. For ground lining interactions, most approaches employ non-tension elastic ground springs. However, these approaches have different methods of evaluating connection joints. Therefore, these theoretical approaches can be classified by joint evaluations [23].

A proper structural model should be selected cautiously to calculate the member forces of the TBM segmental linings since it depends on several factors such as the tunnel usage, design loads, geometry and arrangement of segments, ground conditions, and necessary accuracy of analysis. Schematic diagrams of the structural models outlined by JSCE are shown in Figure 17.

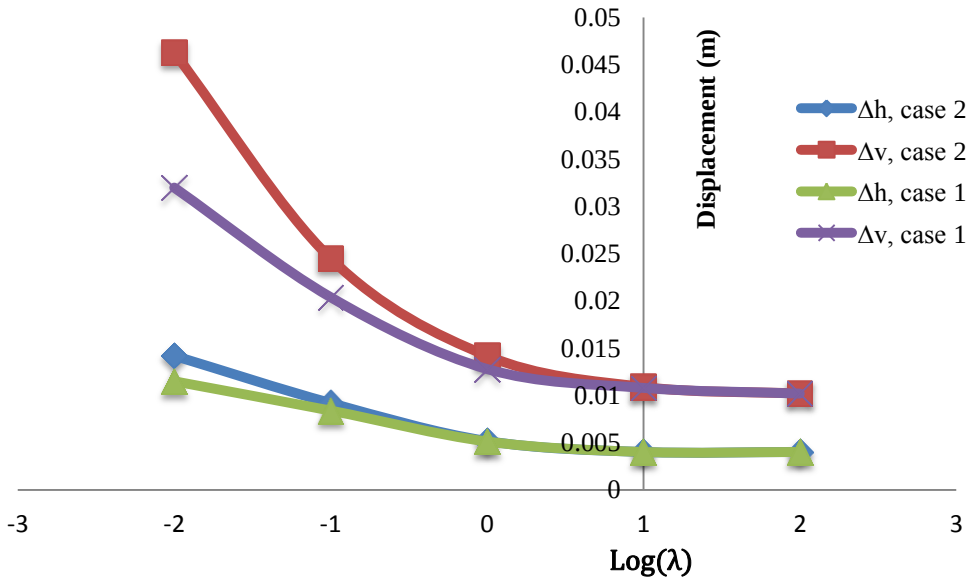


**Figure 15. Variation in lining displacement by different joint arrangements.**

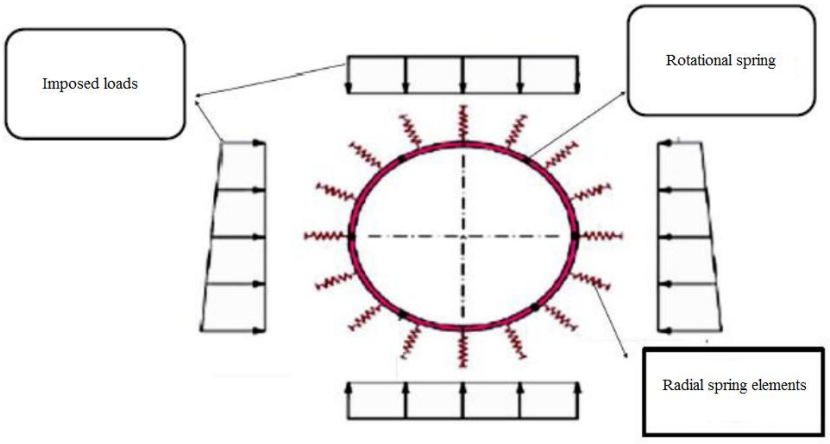


**Figure 16. Model of Beam-Spring method.**

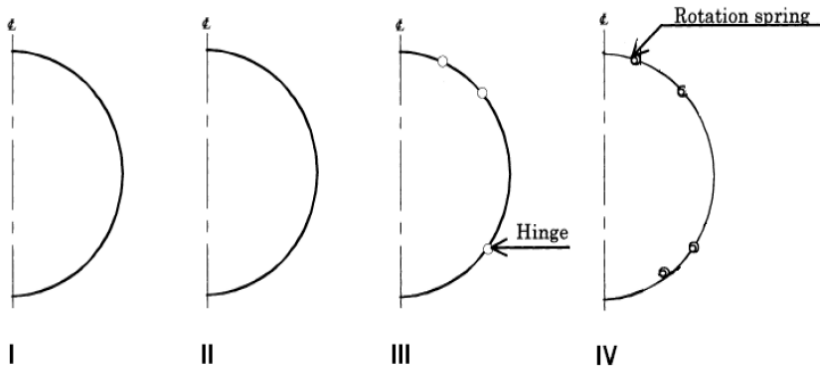


**Figure 17. Structural design models for TBM segmental linings [23].**

The common part of this method is the ground-lining interaction, which is simulated by non-tension elastic ground springs in the radial direction, as shown in Figure 17. The ground spring constant is calculated using the theoretical formulas proposed by Wood as follows [23]:

$$k = \frac{E}{(1+\nu)\times R} \quad (5)$$

where:
$k$ : Modulus of subgrade reaction of ground in radial direction (kN/m$^3$);
$E$ : Modulus of deformation of ground (kN/m$^2$);
$\nu$ : Poisson's ratio;
$R$ : Outer radius of segment (m).

$$k_r = k \times l_s \times w \quad (6)$$

where:
$k_r$ : Rock spring constant in radial direction (kN/m);
$k$ : Modulus of subgrade reaction of ground in radial direction (kN/m$^3$);
$l_s$ : Distance between rock springs (m);
$w$ : Width of segment (m).

In this work, as depicted in Figure 18, rotational springs were established for the expression of joints of lining. To simulate the behavior of rotational stiffness of the longitudinal joints, we used the worldwide accepted formulas proposed by Janssen based on the studies of Leonhardt and Reimann on the resistance against rotation and bending of concrete hinges [24].

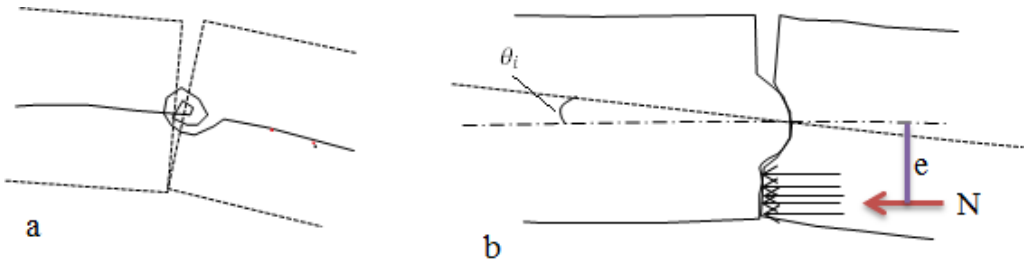


**Figure 18. a) Rotational spring model to simulate lining joints, b) stress distribution at segment joint [25].**

While developing the theoretical formula of Leonhardt and Reimann on concrete joints, the following assumptions were made on the basis of the experimental results and observations of concrete joints.

- Tensile stress is not transmitted at joints.
- Compression stress is linearly distributed.
- The deformation coefficient is constant, with a magnitude of $E_0$ and the initial connection elasticity coefficient of $\sigma = E = 0$.
- The scope of deformation in the acting direction of axial force is centered on the joint surface, and limited to the same scope as the width of the convex potion of the joint. Strain is distributed uniformely [25].

The theoretical formulas based on the above assumptions and the geometric relationships are developed as shown in Figure 19. As long as the joint is fully compressed, the rotational stiffness

remains constant, and can be described by the following formula [23]:

$$k_\theta = b \times (\frac{E \times a^2}{12}) \quad (7)$$

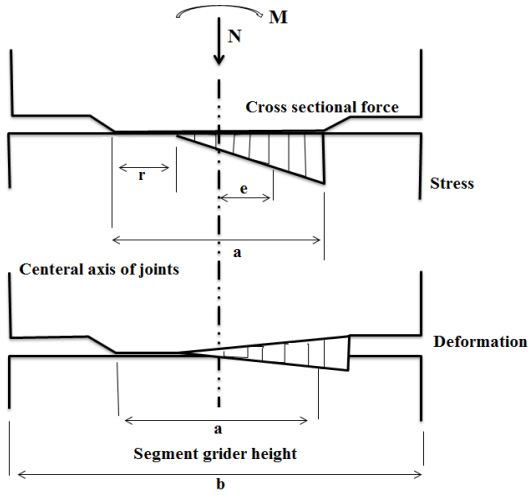


**Figure 19. Stress and deformation in mortised portions [23].**

In this research work, to simulate the behavior of the segmental lining of the Chamshir water conveyance tunnel, a code was established in the MATLAB software based on the Beam-Spring concepts. The tunnel lining was discretized by beam elements connected to each other with nodes that were, in turn, connected to a fixed point by normal and tangential springs, as depicted in Figure 20. This procedure allows cons the interaction of ground and support when the latter is affected by the load-induced deformations. The loads acting on the lining are evaluated by an empirical formulation with respect to the properties of the rock mass and the geometry of the tunnel, as mentioned earlier.

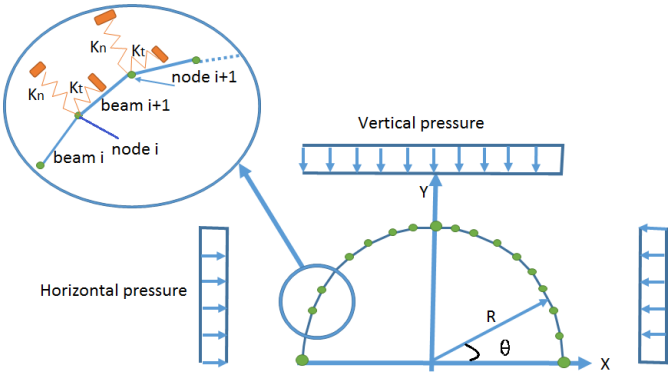


**Figure 20. Layout of the model, horizontal ($q_h$) and vertical loads ($q_v$) and node numbers.**

The beam structural elements are usually modeled as linear elastic, with their stiffness being a function of the thickness and the elastic modulus of the constituting materials. Since the tunnel RC segmental lining is made of concrete and reinforcements (bars and stirrups), it is necessary to define the equivalent tunnel cross-section and a modulus of deformability that take into due account the different properties of concrete and reinforcements. In this work it was assumed that the ground reaction forces were activated when the tunnel expanded outward but they remained inactive when the tunnel contracted inward. Therefore, non-tension (compression only) springs were adopted in the analysis. As mentioned earlier, the ground spring constants are obtained by multiplying the coefficient of subgrade reaction with the tributary area of springs (Eq. 7). Ground springs are placed at each member joint in radial direction so that the number of ground springs will be equal to the number of beam members. The input parameters of this code for generating and computing the internal forces of segmental lining based on the Beam-Spring method are listed in Table 3.

In this part of the work, the Beam-Spring method was utilized to compute the bending moment and axial forces of the Chamshir water conveyance tunnel. The results of the method about the bending moments and axial forces are shown in Figures 21 and 22, respectively.

Also a comparison was made between the computed internal forces from the Force-Method equations and the Beam-Spring method. The results obtained are shown in Figures 23 and 24.

**Table 3. Input parameters of Beam-Spring program to simulate segmental lining behavior.**

| Parameter | Value |
|---|---|
| Number of beams | 30 |
| Number of ground springs | 30 |
| Number of nodes | 60 |
| Length of members ( $l_s$ ) | 225 mm |
| Radius of ring ( $R$ ) | 2150 mm |
| Width of segments | 1200 mm |
| Thickness of segments | 250 mm |
| Moment of inertia of segments | $1.563*10^{-3}\ m^4$ |
| Cross-sectional area of segments | $0.3\ m^2$ |
| Coefficient of subgrade reaction | $36847\ KN/m^3$ |
| Ground spring constant | $9949\ KN/m$ |
| Rotational stiffness | $11354\ KN.m/rad$ |

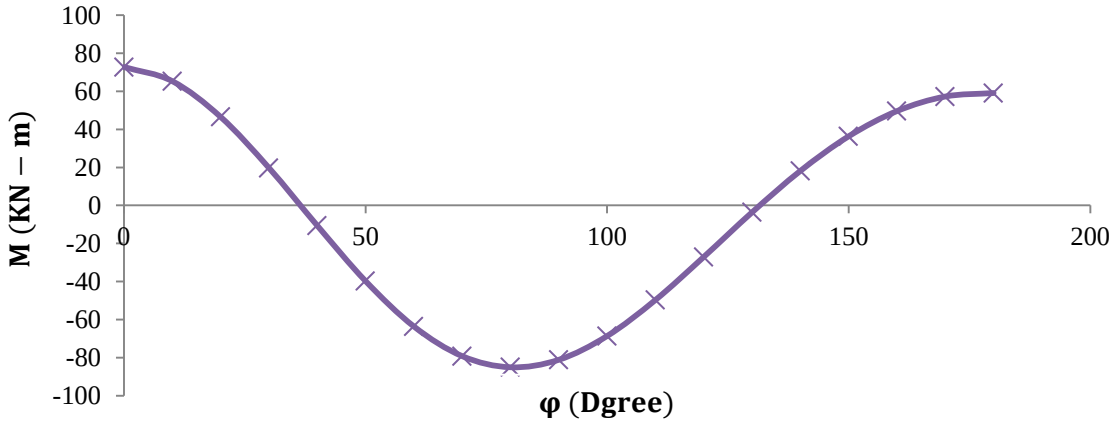


**Figure 21. Bending moment of segmental lining of Chamshir tunnel.**

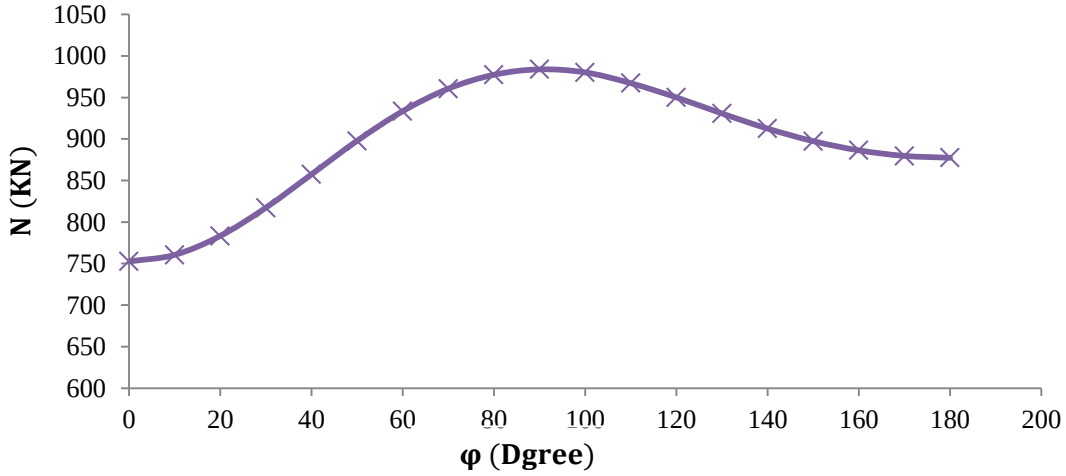


**Figure 22. Axial forces of segmental lining of Chamshir tunnel.**

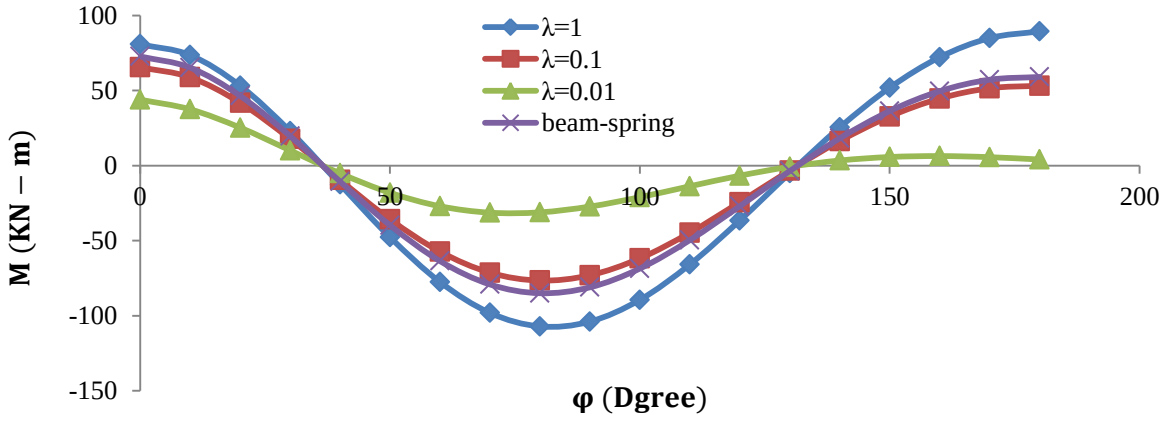


**Figure 23. Comparison between bending moments for different methods.**

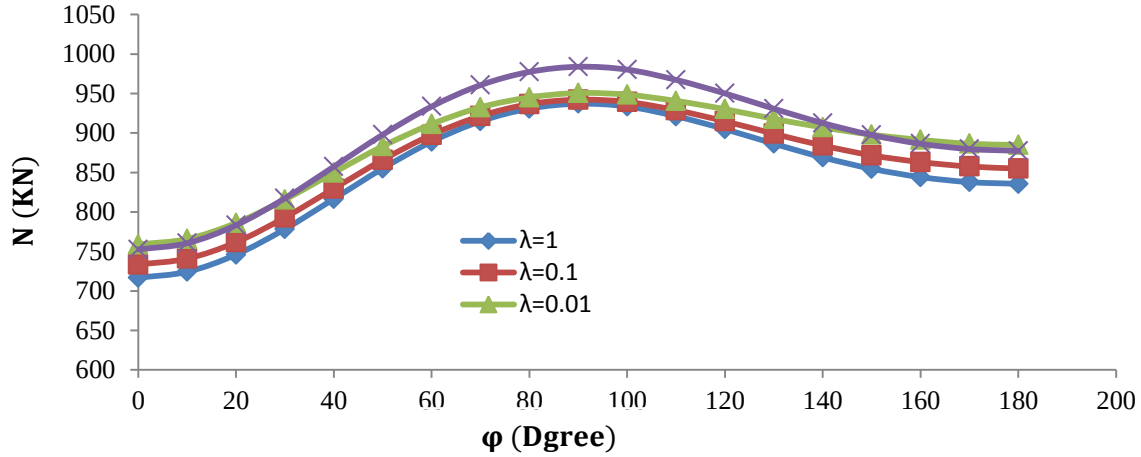


**Figure 24. Comparison between axial forces for different methods.**

As shown in the above figures, when the flextural stiffness of joints is 0.1 ($\lambda = 0.1$), the computed internal forces from the Beam-Spring method will be close to the internal forces computed from the Force-Method equation.

The effect of joint arrangements and rotational stiffness of springs on the beam spring analysis is presented in the following sections.

### 3.1. Effect of joints arrangements on Beam-Spring analysis

In this part of the work, three probable joint arrangements, (Guray, 2010) were examined by the Beam-Spring method for a segmental lining sequence to determine the effect of lining joint arrangements on the internal forces. The following joint arrangement patterns were considered:

Pattern one: 22.7, 81.5, 140.3, 199.1, 257.9, 316.7, 323.9 degrees.

Pattern two: 15.5, 74.3, 133.1, 191.9, 250.7, 309.5, 316.7 degrees.

Pattern three: 37.1, 95.9, 154.7, 213.5, 272.3, 331.3, 338.3 degrees.

The imposed bending moments and axial forces of segmental lining for the above patterns are shown in Figures 25 and 26, respectively.

As it can be seen, when the first joint is positioned near the crown, the bending moment is lower than the other states. On the other word, when the first joint is placed near the crown, the axial forces will be greater than the other states but the increased rate of bending moment is more than the reduced rate of axial forces under this situation.

The results obtained show that the lining joint arrangement in sequential rings is another geometrical parameter that affects the internal forces, especially bending moments. For this reason, different lining joint patterns for a ring should be analyzed to determine the optimal segment arrangement in the design of segmental linings.

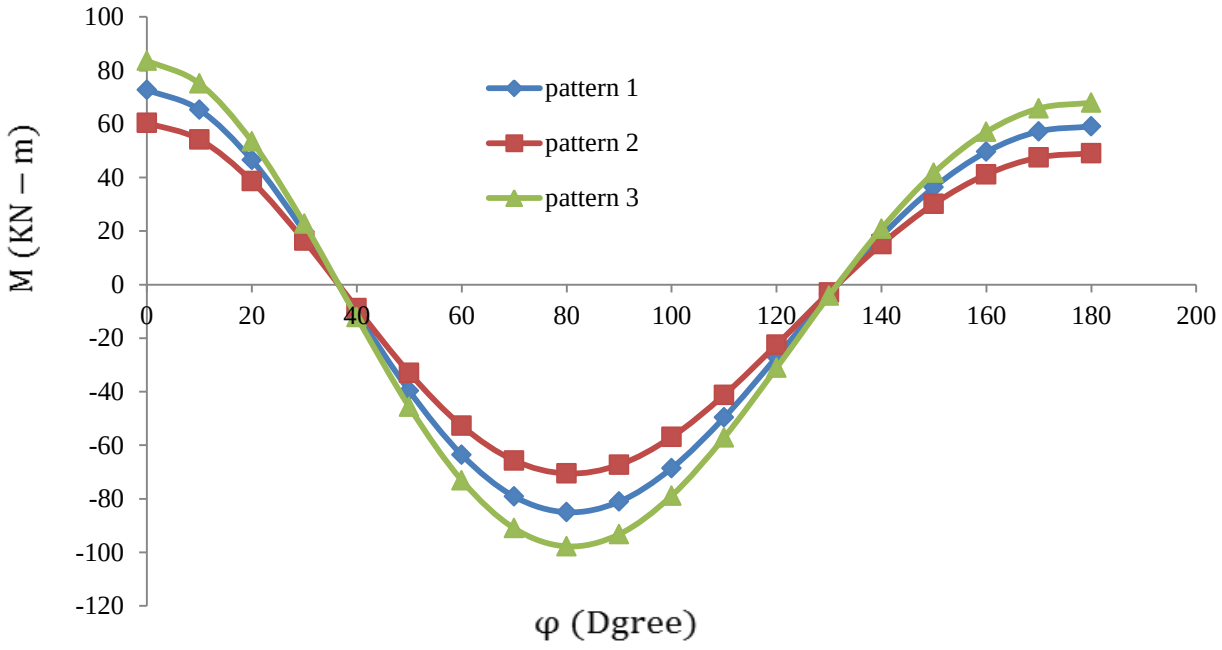


**Figure 25. Variation in imposed bending moment versus joint arrangements.**

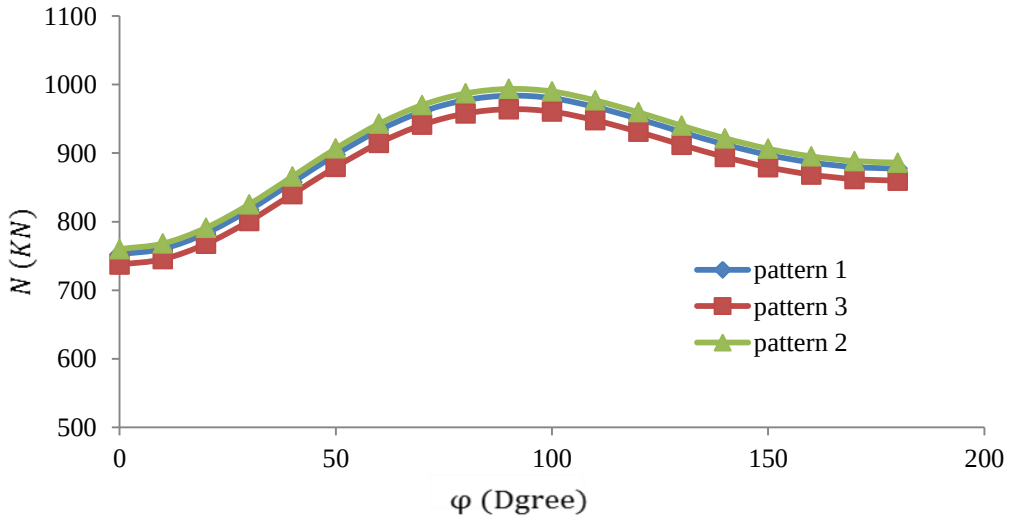


**Figure 26. Variation in imposed axial forces versus joint arrangements.**

### 3.2. Effect of rotational stiffness on Beam-Spring analysis

To determine the sensitivity of the rotational spring constants, three Beam-Spring models with different rotational spring constants were employed. Moreover, the bending moment and axial force changes with respect to this parameter are depicted in Figures 27 and 28, respectively.

As shown in the above figures, the Beam-Spring model with the highest rotational spring constant yields the maximum results for the bending moment and axial forces. It is because an increase in the rotational spring constant leads to a hike in the load transfer between segmental pieces. Therefore, a higher load transfer raises the internal forces. It could be concluded that the rotational spring constant, which is a mechanical property of the segmental lining joints, has a remarkable effect on the imposed internal forces, especially on bending moment. Therefore, selecting a realistic rotational spring constant is essential for the Beam-Spring analysis.

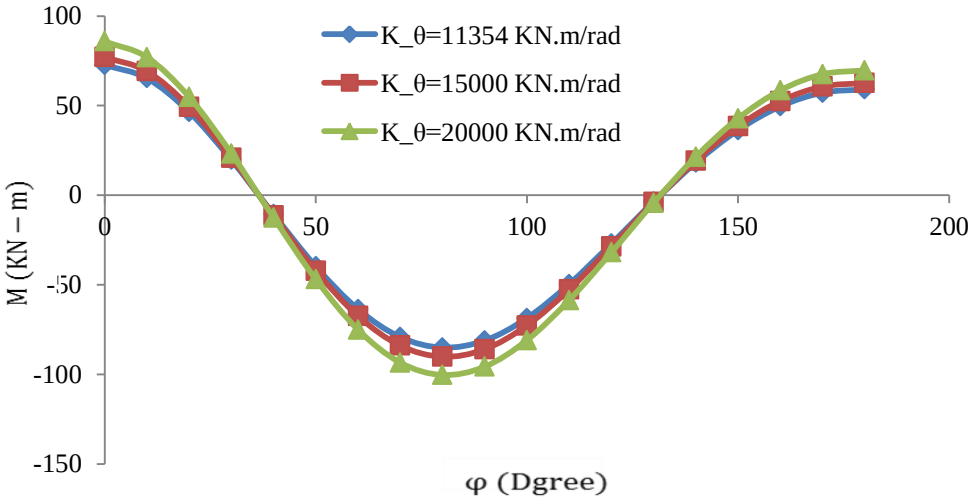


**Figure 27. Variation in imposed bending moment by rotational spring constant.**

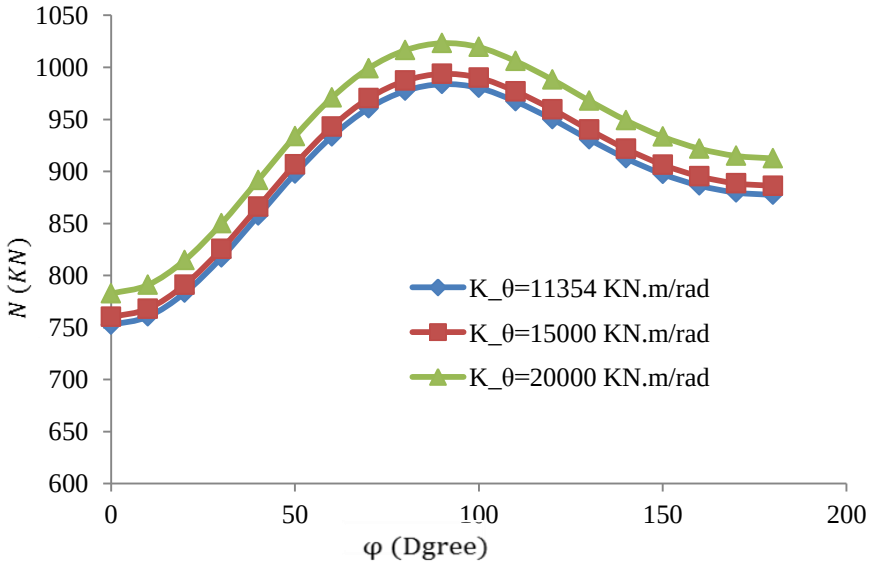


**Figure 28. Variation in imposed axial forces by rotational spring constant.**

## 4. Structural design of Chamshir tunnel segmental lining

For a segmental lining design, the nominal strength of lining should be decreased by a coefficient of ($\phi$). The diminished strength of lining should be able to resist the imposed forces, according to the following equation:

$$\phi S_n \geq \beta P \tag{8}$$

The interaction curve of lining shows the acceptable combination of bending moment and axial forces in the reinforced or unreinforced concrete. The stress distribution on the section of lining is depicted in Figure 29. As it can be seen, the combined yield forces consisting of bending moment and axial forces could be determined by the following equation:

$$P_n = C_S + C_C - T_S$$
$$M_n = C_S \times \left(\frac{H}{2} - d'\right) + C_C \tag{10}$$
$$\times \left(\frac{H}{2} - \frac{a_b}{2}\right) + T_S \times \left(d'' - \frac{H}{2}\right)$$

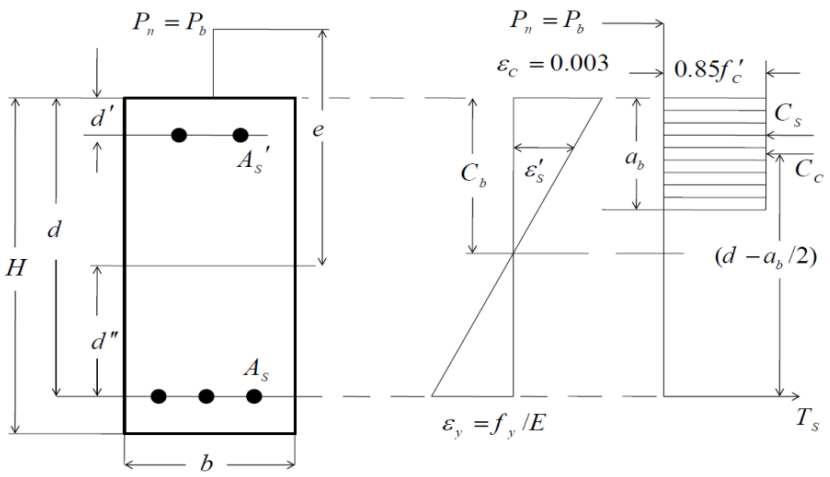


**Figure 29. Stress distribution curve of lining section [26].**

where

$T_S = A_S.F_y$ , and $C_C = 0.85 f_C.b.a_b$ ,

$C_S = A_S.f_y$ .

For a stability evaluation of the reinforced concrete section, the correlated bending moments and axial forces must be incorporated in the interaction diagram. By considering this approach, the stability of the selected segmental lining was analyzed at the critical sections of the tunnel. The results of this evaluation are depicted in Figure 30.

According to these results, all the combined bending moments and axial forces are placed inside the interaction curve of the segmental lining region. As a result, the selected design specifications of the segmental lining should be able to resist the internal forces, with an acceptable safety factor.

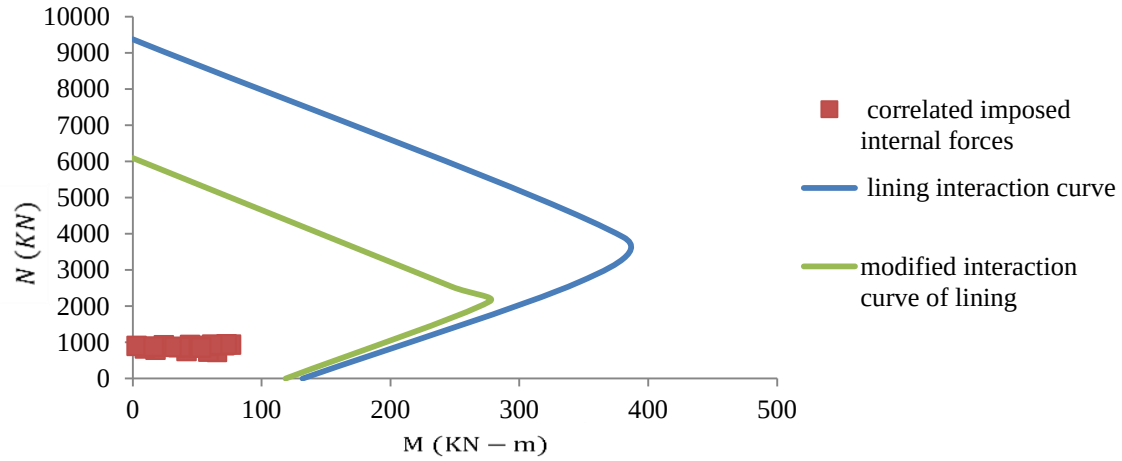


**Figure 30. Segmental lining interaction curve of Chamshir tunnel.**

## 5. Conclusions

The results of this research work could be summarized as follows:

- According to the Force-Methods equation, the bending moment is reduced when the joint stiffness coefficient is lower than 1. However, when the rigidity of joints of segment rises, the lining behaves like a continuous lining without any joints. Hence, the bending moment increases as well. Also the axial forces of lining rise until the joint stiffness coefficient is lower than 1, and with an increase in it, the vertical and horizontal displacements of segmental lining are increased.
- According to the Force-Methods equation, as the soil resistance coefficient ($K_S$) increases, the bending moments and the

axial forces of segmental lining are increased and decreased, respectively.

- The results obtained show that an increase in the joint number leads to a hike in the flexibility of segmental lining, and consequently, a decline in the bending moments. However, it raises the segmental lining deformations and ground reaction pressure. As a result, the axial forces, extremely affected by pressure, are increased.
- This study revealed that an increase in the amount of lining joint angle (regarding the tunnel crown) led to the rise and fall of the bending moment and axial forces, respectively. Hence, when the first position of lining joint is placed near the tunnel crown, the arrangements of lining will be optimal from a structural viewpoint.
- A comparison between the internal forces achieved from Force-Method and Beam-Spring method suggests that the flexural stiffness of joints is 0.1 ($\lambda = 0.1$), i.e. the internal forces computed from the Beam-Spring method resemble the internal forces computed from the Force-Method equation, which reveal that, unlike the literature ([10], [15], [19]), the results of the direct methods (such asthe Force Method) could be more realistic when the tunnel is excavated at a high depth within the rock medium in the case of a symmetrical joint distribution.
- An increase in the amount of the rotational stiffness of springs leads to a hike in the bending moments and axial forces.
- By drawing a interaction diagram for the proposed segmental lining pattern for the Chamshir tunnel, the bending moments and axial forces were both plotted inside the interaction curve, meaning that the suggested segmental lining pattern is secured with an acceptable safety factor.

## References

[1]. Kim, H.J. and Eisenstein, Z. (2006). Prediction of Tunnel Lining Loads Using Correction Factors. Engineering Geology. 85 (3-4): 302-312.

[2]. Kim, S.H., Pelizza, S. and Kim, J.S. (2006). A study of Strength Parameters in the Reinforced Ground by Rock Bolts. Tunneling and Underground Space Technology. 21(3-4): 378-379.

[3]. Wood, A.M. (1975). The Circular Tunnel in Elastic Ground. Geotechnique. 25 (1): 115-127.

[4]. Bickel, J.O., Kuesel, T.R. and King, E.H. (1996). Tunnel Engineering Handbook, Chapman & Hall, United States of America.

[5]. Koyama, Y. and Nishimura, T. (1998). Design of Lining Segment of Shield Tunnel Using a Beam – Spring Model, Quarterly Report of Railway Technical Research Institute. 39 (1).

[6]. Mashimo, H. and Ishimura, T. (2003). Evaluation of the Load on a Shield Tunnel Lining in Gravel, Public Works Research Institute, Independent Administrative Institution, Tsukuba, Japan.

[7]. Lee, K.M. and Ge, X.W. (2001). The Equivalent of the Jointed Shield Driven Tunnel Lining to a Continuous Ring Structure. Canadian Geotechnical Journal. 38(3): 461-483.

[8]. Lee, K.M., Hou, X.Y., Ge, X.W. and Tang, Y. (2001). An Analytical Solution for a Jointed Shield-Driven Tunnel Lining. International Journal for Numerical and Analytical Methods in Geomechanics. 25 (4): 365-390.

[9]. Koyama, Y. (2003). Present Status and Technology of Shield Tunneling Method in Japan. Tunneling and Underground Space Technology. 18 (2-3): 145-159.

[10]. Lu, L., Lu, X. and Fan, P. (2011). Full-Ring Experimental Study of The Lining Structure of Shanghai Changjiang Tunnel. Civil Engineering and Architecture. 45 (8): 732-739. ISSN:1934-7359.

[11]. Teachavorasinskun, S. and Chub-uppakarn, T. (2010). Influence of Segmental Joints on Tunnel Lining. Tunneling and Underground Space Technology. 25 (4): 490-494.

[12]. Arnau, O. and Molins, C. (2012). Three dimensional structural response of segmental tunnel linings, Engineering Structures. 44: 210-221.

[13]. Arnau, O. and Molins, C. (2011a). Experimental and analytical study of the structural response of segmental tunnel linings based on an in situ loading test. Part 1: Test configuration and execution. Tunneling and Underground Space Technology. 26: 764-777.

[14]. Arnau, O. and Molins, C. (2011b). Experimental and analytical study of the structural response of segmental tunnel linings based on an in situ loading test. Part 2: Numerical simulation. Tunneling and Underground Space Technology. 26: 778-788.

[15]. Do, N. and Dias, D. (2012). 2D numerical investigation of segmental tunnel lining behavior. Tunneling and Underground Space Technology. 37: 115-127.

[16]. Li, X. and Yan, Z. (2015). Experimental and analytical study on longitudinal joint opening of concrete segmental lining. Tunneling and Underground Space Technology. 46: 52-63.

[17]. Zhong, X., Zhu, W., Huang, Z. and Han, Y. (2006). Effect of joint structure on joint stiffness for shield tunnel lining. Tunneling and Underground Space Technology. 21: 406- 407.

[18]. Yu, H.T., Yuan, Y., Qiao, Z.Z., Gu, Y., Yang, Z.H. and Li, X.D. (2013). Seismic analysis of a long tunnel based on multi-scale method. Engineering Structure. 49: 572-587.

[19]. El Naggar, H. and Hinchberger, S.D. (2008). An analytical solution for jointed tunnellinings in elastic soil or rock. Canadian Geotech. Journal. 45 (11): 1572-1593.

[20]. Iranian Oil Operating Companies (IOOC). (1996). Gachsaran Geological Map. 1: 100,000.

[21]. AFTES – WG7, Considerations on the Usual Methods of Tunnel Lining Design. (1993). French Tunneling and Underground Engineering Association, Working Group No. 7 - Temporary Supports and Permanent Lining.

[22]. JSCE, Japanese Standard for Shield Tunneling.(1996). Japan Society of Civil Engineers, The third edition, Tokyo.

[23]. Guray, A. (2010). Evaluation of structural analysis used for the design of TBM segmental linings, Master thesis of civil engineering, Middle East Technical University.

[24]. Klappers, C., Gruebl, F. and Ostermeier, B. (1999). Structural Analysis of Segmental Lining – Coupled Beam and Spring Analyses Versus 3D FEM Calculations with Shell Elements, Tunneling and Underground Space Technology. 21 ( 3-4).

[25]. Wang, J.J. (2005). The Design Considerations for the Segmental Lining of the Hsuehshan Tunnel, International Symposium on Design, Construction and Operation of Long Tunnels, Taiwan.

[26]. Tahouni, S. (2004). Reinforce concrete structure design. (in Persian).

# ارزیابی تحلیل سازه‌ای پوشش سگمنت بتنی پوشش تونل با استفاده از روش فنر- میله و روش- نیرو (مطالعه موردی: تونل انتقال آب چم شیر)

**مجید نیکخواه*[۱]، سید سعید موسوی [۱]، شکرالله زارع[۱] و امید خادم حسینی[۲]**

**۱- دانشکده مهندسی معدن، نفت و ژئوفیزیک، دانشگاه صنعتی شاهرود، ایران**

**۲- دانشکده مهندسی عمران، دانشگاه صنعتی شاهرود، ایران**

ارسال ۲۰۱۵/۱۱/۲۰، پذیرش ۲۰۱۶/۱/۲۵

* نویسنده مسئول مکاتبات: m.nikkhah@shahroodut.ac.ir

**چکیده:**

اتصالات و درزهای بین سگمنت‌های پوشش بتنی تونل‌ها می‌توانند مقدار مشخصی ممان خمشی، نیروهای محوری و برشی را تحمل نمایند. به طور کلی در طراحی سازه‌ای سگمنت‌های بتنی تونل‌ها، اتصالات به صورت لولاهای الاستیک و فنرهای دورانی مدل شده و صلبیت آن‌ها باید برحسب صلبیت اتصالات یا سختی‌های دورانی بیان شوند؛ بنابراین ممان خمشی وارد بر پوشش بتنی می‌توانند کاهش یابند و در نتیجه طراحان تونل برای انتخاب قطعات پوشش بتنی با هزینه کمتر آزادی عمل بیشتری خواهند داشت. در این تحقیق، تحلیل سازه‌ای قطعات پیش‌ساخته بتنی تونل با توجه به تغییرات سختی خمشی اتصالات، ضریب مقاومت خاک، تعداد اتصالات قطعات پوشش بتنی و آرایش اتصالات سگمنت‌ها با استفاده از معادلات روش-نیرو انجام گرفته است. سپس ممان خمشی و نیروهای محوری ایجاد شده توسط روش فنر- میله که به طور وسیعی در تحلیل‌های نیروهای داخلی قطعات پوشش بتنی بکار می‌روند محاسبه گردیده و با نتایج حاصل از معادلات روش-نیرو مقایسه شده‌اند. در ادامه اثرات الگوی آرایش اتصالات و سختی فنر دورانی با توجه به نتایج به دست آمده از تحلیل فنر-میله ارزیابی شده است. در نهایت مشخصه‌های بهینه طراحی قطعات پوشش بتن مسلح با استفاده از دیاگرام اندرکنش ممان‌های خمشی و نیروهای محوری مورد بررسی واقع شده‌اند. نتایج به دست آمده نشان می‌دهند که الگوی ارائه شده برای سگمنت‌های بتنی پوشش تونل انتقال آب چم شیر (به عنوان یک مطالعه موردی) در مقابل با فشارهای خارجی وارد بر قطعات پوشش بتنی، در وضعیت ایمنی قابل قبولی قراردادند.

**کلمات کلیدی:** تونل، طراحی سگمنت پوششی، تحلیل سازه‌ای، روش فنر- میله، تونل چم شیر.